The Open-Circuit Ennoblement of Alloy C-22 and Other Ni-Cr-Mo Alloys

A.C. Lloyd, J.J. Noël, N.S. McIntyre, and D.W. Shoesmith

The open-circuit corrosion and anodic oxidation behavior of the C-series of Ni-Cr-Mo alloys (C-4, C-276, C-2000, and C-22) and alloy 625 have been studied at 25°C and 75°C in 1.0 mol·L^{-1} NaCl + 1.0 mol·L^{-1} H_2SO_4. A combination of open-circuit potential, potentiostatic polarization, and electrochemical impedance spectroscopy were employed in the study. The composition of the films formed was determined by x-ray photoelectron spectroscopy and time-of-flight secondary ion mass spectrometry. Passive oxide film resistances increase and defect oxide film concentrations decrease as films thicken and chromium and molybdenum segregate to the alloy/oxide and oxide/solution interfaces, respectively. The high-chromium alloys exhibit higher film resistances and lower film defect concentrations consistent with the more positive potentials observed on these alloys. The results show that the observed ennoblement in corrosion potentials with time is coupled to the Cr/Mo segregation process and the suppression of defect injection at the alloy/oxide interface. By all measures, C-22 exhibited the best passive properties.

INTRODUCTION

An Ni-Cr-Mo alloy, alloy 22, is the candidate material for the outer shell of the high-level nuclear waste packages proposed for disposal of wastes within the Yucca Mountain repository in Nevada.[1] Providing that localized corrosion can be shown to be unlikely under repository conditions, the long-term corrosion performance (over 10,000 years) of the package will be determined by the passive corrosion behavior of this alloy. How the passive behavior evolves with changes in temperature and redox conditions, which will change considerably over the lifetime of the waste package, will dictate the corrosion resistance of the container. Accordingly, temperature and redox potential represent two important determinants of waste package performance.

The use of an Ni-Cr-Mo alloy, such as alloy 22, for the design of the waste package container is supported by electrochemical evidence, which shows that chromium additions to nickel result in a narrower active region, a lower passive current density, and a wider passive potential range.[2,3] This enhanced passivity is generally attributed to a higher concentration of Cr(III) in the inner oxide layer than in the substrate alloy[4] due to the growth and defect annealing of a Cr(III) oxide barrier layer at the alloy/oxide interface. X-ray photoelectron spectroscopy (XPS) and scanning-tunneling microscopy (STM) have shown that the passive film (on Cr, Fe-Cr, Fe-Cr-Ni, and Ni-Cr metals and alloys) consists primarily of an inner layer of Cr_2O_3 and an outer layer of $Cr(OH)_3$.[5–7]

While the synergistic effect of alloying molybdenum with chromium in nickel-based alloys is well known, the specific role molybdenum plays in the passive corrosion behavior remains an area of debate. The presence of molybdenum in oxide films has been established for alloys containing high amounts of molybdenum.[8] In ferrous alloys, molybdenum is thought to enhance the dissolution rate by facilitating the selective dissolution of iron through the passive film. It has been suggested that Mo(IV) replaces Cr(III) in the passive film while Mo(VI) is segregated to the outer regions of the film.[9] According to Bojinov et al.,[10] Mo(IV) increases the overall degree of non-stoichiometry in the film, which enhances the generation of oxygen vacancies and thereby the dehydration of the chromium oxide inner boundary layer.[10,11] A review of other hypotheses has been given by Clayton and Olefjord.[12]

Recently, Bojinov et al. developed the mixed conduction model (MCM) for oxide growth on passive alloys.[10,13–15] In this model, film growth occurs by the transport of point defects that act as electron donors or acceptors. Each defect coexists with an electronic defect that

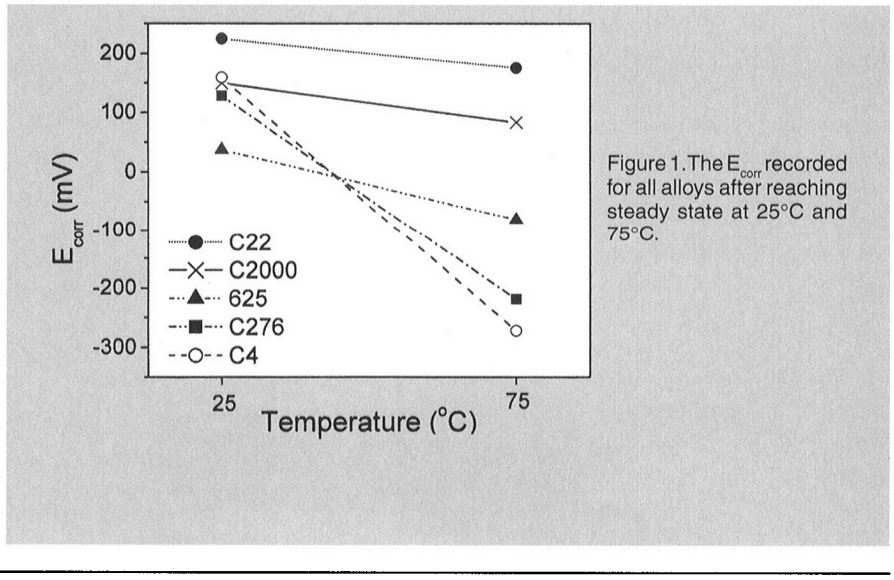

Figure 1. The E_{corr} recorded for all alloys after reaching steady state at 25°C and 75°C.

EXPERIMENTAL PROCEDURES

Nominal alloy compositions are given in Table A. Cylindrical samples (1 cm in diameter and height) were cut, and the connecting rod, connection point, and top of the electrode were painted with a water- and heat-resistant sealant (Sealit). To avoid crevices, this contact was not immersed in solution. The electrodes were wet-polished to a 1 μm finish, immediately rinsed with methanol, ultrasonically cleaned in ultra-high-purity argon-deaerated deionized water for ~10 s, and quickly immersed in the deaerated 1.0 mol·L^{-1} NaCl + 0.1 mol·L^{-1} H_2SO_4 solution.

After establishment of a steady-state corrosion potential (E_{corr}) at 25°C, an electrochemical impedance spectrum (EIS) (10^5–10^{-2} Hz) was recorded. The temperature was raised to 75°C and the E_{corr}/EIS sequence repeated. A potential of 350 mV was then applied for 3 days at 75°C. After polarization, E_{corr} was again recorded, and a final EIS taken. Each specimen was then rinsed in ultra-pure deionized water and analyzed using x-ray photoelectron spectroscopy (XPS) and time-of-flight secondary ion mass spectrometry (TOF SIMS). The details of the XPS and TOF SIMS experimental procedures have been published elsewhere.[17] All potentials were measured against an Ag/AgCl (0.1 mol·L^{-1} KCl) reference electrode and are quoted against this scale.

Table A. Nominal Chemical Compositions of the Alloys under Investigation

	Nominal Composition of Alloys (wt.%)				
Alloying Element	C-22 NO6022	C-2000 NO6200	625 NO6625	C-276 N10276	C-4 NO6455
Ni	56**	59**	62**	57**	65**
Cr	22	23	21	16	16
Mo	13	16	9	16	16
W	3	—	—	4	—
Fe	3	3*	5*	5	3*
Co	2.5*	2*	1*	2.5*	2*
Mn	0.5*	0.5*	0.5*	1*	1*
Si	0.08*	0.08*	0.5*	0.08*	0.08*
C	0.01*	0.01*	0.1*	0.01*	0.01*
Cu	—	1.6	—	—	—
S	0.02*	0.01*	0.02*	0.02*	0.03*
Nb			4		

** As balance
* As maximum

contributes to the conductivity of the film. Electron acceptors are the cation vacancies generated at the film/solution interface (the major negative charge carriers), while donors are the metal interstitials and/or oxygen vacancies generated at the metal/film interface (major positive charge carriers). The conductivity of an oxide film in contact with an electrolyte is determined by the quantity and mobility of ionic defects.

Based on the MCM, the total impedance of a passive system (Z_T) can be represented by the sum of the film and interfacial impedances acting in series,[16]

$$Z_T = Z_{M/O} + Z_F + Z_{O/S} \quad (1)$$

where $Z_{M/O}$ represents the impedance across the alloy/oxide interface, $Z_{O/S}$ is impedance across the oxide/solution interface, and Z_F is the film impedance. There are two contributions to Z_F. One is Z_{VM}, the impedance to vacancy migration in response to the electric field across the oxide. The other is Z_{DT}, the impedance to the diffusive transport of defects due to the presence of gradients in defect concentrations, as shown in Equation 2.

$$Z_F = Z_{VM} + Z_{DT} \quad (2)$$

Z_{VM} will always contribute to Z_T since an electrical field will always be present across the oxide. By contrast, Z_{DT} should be negligible if the film contains only a small concentration of defects. Z_{DT} would have the form of a Warburg impedance and, if present, would influence the low frequency range of the impedance spectrum. For sufficiently low defect concentrations and/or values of diffusion coefficient, this Warburg response may only be detectable at frequencies below the measurable frequency range.

This theory links the electrical and electrochemical properties of passive films on Ni-Cr-Mo alloys to the rate of the transfer of charged species through the film and across the interfaces. An understanding of the passive corrosion behavior of an alloy such as alloy 22 must therefore be determined in terms of the transport mechanisms through which changes in composition, structure, and overall stability of the film are governed. The sidebar provides experimental details for a series of experiments that were used to illustrate the influence of oxide composition on film impedance and ennoblement properties.

RESULTS

The steady-state E_{corr} values (after 2 to 3 days) at 25°C and 75°C are shown for all alloys in Figure 1. Upon heating to 75°C, E_{corr} initially dropped for all alloys, but recovered eventually only for C-22 and C-2000. For C-276 and

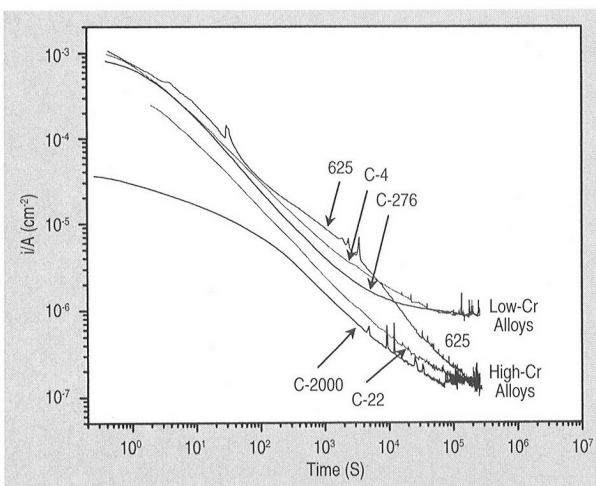

Figure 2. The current response for all alloys during polarization at 350 mV, in 1.0 mol·L^{-1} NaCl + 0.1 mol·L^{-1} H_2SO_4 at 75°C.

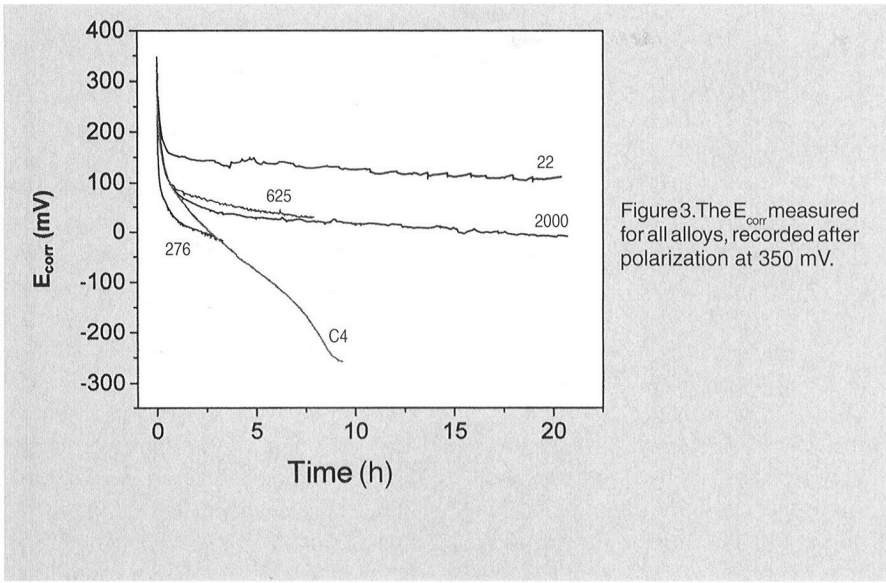

Figure 3. The E_{corr} measured for all alloys, recorded after polarization at 350 mV.

C-4, E_{corr} did not recover, having rapidly achieved lower steady-state values. E_{corr} for 625 exhibited intermediate behavior, indicating that a high chromium content alone is insufficient to drive the potential to the positive values exhibited by C-22 and C-2000.

Figure 2 shows the current-time transients recorded for each alloy at 350 mV. The difference in behavior between the high- and low-chromium alloys is clear. The passive currents for C-276 and C-4 achieved a steady-state value significantly higher than the final, non-steady-state currents measured on C-22, C-2000, and 625. Despite differences at short times, the currents for these last three alloys approach similar values at longer times. Only a small fraction (<1%) of the total charge is utilized in film growth. The remainder of the charge goes to metal dissolution,[18] and the apparent absence of steady state for the high-chromium alloys suggests the film growth/defect annealing process is incomplete.

Subsequent to anodic polarization, E_{corr} for C-22 and C-2000 stabilized at values close to those measured prior to polarization (Figure 3), indicating the presence of stable passive films. By contrast, E_{corr} for C-276 and C-4 relaxed to less positive values, suggesting the anodic films were not stable at 75°C in this environment. The stable higher E_{corr} after anodic oxidation demonstrates the improved behavior of 625 due to the anodic treatment.

Following the electrochemical experiments, XPS and time-of-flight secondary ion mass spectrometry (TOF SIMS) were used to determine the general oxide composition and to profile the distribution of metal cations within the oxide, respectively. In previous studies and other published literature, it has been observed that chromium and nickel concentrate at the alloy/oxide interface, while molybdenum and tungsten are enriched in the outer surface of the film.[6,17] The degree of segregation between Cr/Ni and Mo/W observed for these alloys (from TOF SIMS) is shown in Figure 4, which shows the Cr/Mo intensity ratio as a function of depth into the oxide for each alloy. The calculation of this ratio was terminated at the alloy/oxide interface. Figure 4 clearly shows that the high-chromium alloys grew the thicker oxide films and, in so doing, achieved the highest Cr/Mo ratios at the alloy/oxide interface. The films on the low-chromium alloys did not grow as thick or achieve as high a level of Cr/Mo segregation. This is particularly obvious for C-4, which grew only a very thin oxide film with negligible Cr/Mo segregation.

The approximate compositions of the oxide films on each alloy were calculated from the XPS spectra using the area counts (using the Scofield cross section[19] and correcting for the relative sensitivity factors) for chromium oxides in the chromium 2p peak, nickel oxide in the nickel 3p peak, all the molybdenum oxides from the molybdenum 3d peak, and tungsten oxides in the tungsten 4f peak (C-22 and C-276). Figure 5 gives the results of this analysis and shows that C-22, C-2000, and 625 had similar oxide compositions with an enrichment of chromium and molybdenum in the film compared to their bulk concentration in the alloy. The chromium enrichment, ~65%, was particularly marked for the high-chromium alloys. Alloy 625 showed slightly lower molybdenum and higher chromium and nickel contents than C-22 and C-2000, consistent with the lower bulk molybdenum content of the alloy. C-4, with the poorest response to anodic oxidation, had a significantly lower chromium content accompanied by a higher molybdenum oxide content, consistent with the low Cr/Mo ratios observed by TOF SIMS. Since the only major difference in bulk compositions between C-4 and C-276 is their tungsten content, this suggests a role for tungsten in maintaining passivity by enforcing growth of a chromium-rich region at the alloy/oxide interface under oxidizing conditions.

These surface analyses are consistent with electrochemical measurements,

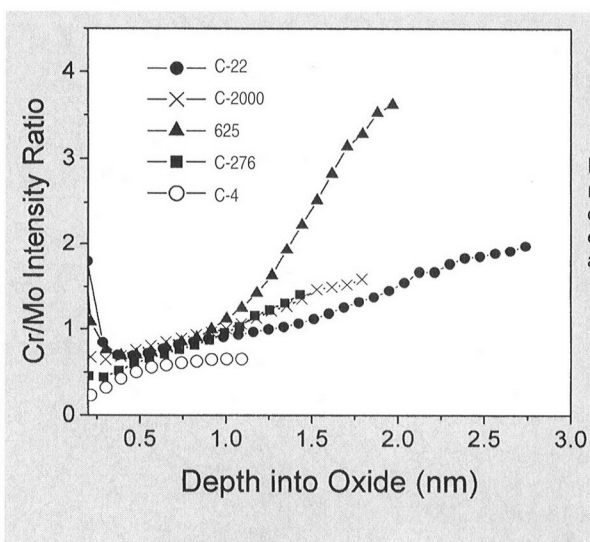

Figure 4. The Cr/Mo intensity ratios from the TOF SIMS profiles obtained upon completion of the electrochemical experiment for all alloys.

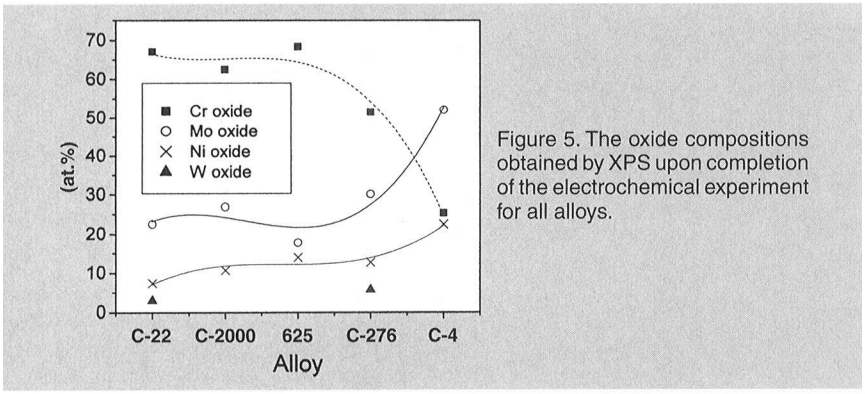

Figure 5. The oxide compositions obtained by XPS upon completion of the electrochemical experiment for all alloys.

which showed that the high-chromium alloys were able to reach, and in the case of C-22 and C-2000, maintain, stable positive E_{corr} values and low passive currents (Figures 1 to 3).

The E_{corr} values measured at 25°C and 75°C range from noble (passive) potentials (C-22 and C-2000 in Figure 1), to negative potentials (C-4 and C-276 in Figure 1) that approach the active region.[17] Thus, the electrochemical impedance spectra (EIS) obtained under steady-state E_{corr} conditions at 25°C, 75°C, and on relaxation after anodic oxidation (Figure 3) span a wide section of the passive region. Film resistance (R_{film}) and capacitance (C_{film}) values were determined by fitting the EIS according to the reasoning outlined previously. Figure 6 shows that there is a relationship between E_{corr} and the electronic properties of the films. There is also an apparent correlation between the resistance of the oxide film (R_{film}) and the capacitative properties (C_{film}). The increase in R_{film} as C_{film} decreases has also been observed during polarization experiments performed by Bojinov et al. on Fe-Cr and Ni-Cr alloys.[13–15]

DISCUSSION

According to Equation 3, capacitance is proportional to the polarizability of the oxide film,

$$C = \frac{\varepsilon\varepsilon^{o}}{d} \qquad (3)$$

where ε is the dielectric constant, ε^{o} is the permittivity of free space, and d is the thickness of the oxide film. A decrease in the capacitance (C) may result from either an increase in the film thickness or a decrease in the dielectric constant. An increase in the dielectric constant is consistent with an increase in the defect density within the oxide film and would be expected to be accompanied by a decrease in R_{film}.[16] By this argument, Figure 6 suggests that a more noble E_{corr} indicates a less defective (and therefore highly resistive) oxide film. Inspection of the upper portion of Figure 6 shows that R_{film} for the three high-chromium alloys, especially C-22 and C-2000, changes very little with changes in temperature. The higher values of C_{film} and lower values of R_{film} for C-4 and C-276 at negative values of E_{corr} are consistent with the presence of a higher concentration of defects. The dependencies of R_{film} and C_{film} on potential are consistent with the expectations of the MCM. For potentials toward the negative end of the passive region, the primary defect is most likely to be an oxygen vacancy (O_V). As the potential is increased and the potential drop across the alloy/oxide interface decreases, this theory predicts a decrease in the number density of defects, as observed in this study.

The main contribution to R_{film} comes from that part of the film with the lowest defect concentration and conductivity.[13–16] Thus, the observation of a high concentration of chromium at the alloy/oxide interface for the high-chromium alloys (Figures 3 and 4) suggests that the ennoblement of E_{corr} is enforced by the Cr/Mo segregation process. It also suggests that the low-chromium alloys, C-276 and especially C-4, do not experience or maintain segregation after an increase in temperature under open-circuit corrosion conditions, as observed. This lack of a chromium inner-barrier layer allows the generation of a large number of defects, leading to a significant increase in film conductivity (Figure 6). By contrast, the formation of an inner barrier layer of chromium slows down the transport of defects and their rate of injection at the alloy/oxide interface for the high-chromium alloys. However, a high chromium content in the alloy, on its own, does not lead to optimized film properties, as indicated by the intermediate behavior of 625.

The results in Figure 6 have significant implications when considering the ennoblement process that occurs on these alloys under open-circuit corrosion conditions. The generally accepted criterion for defining the susceptibility of a metal or alloy to localized corrosion in a specific exposure environment is defined by the relationship between E_{corr}

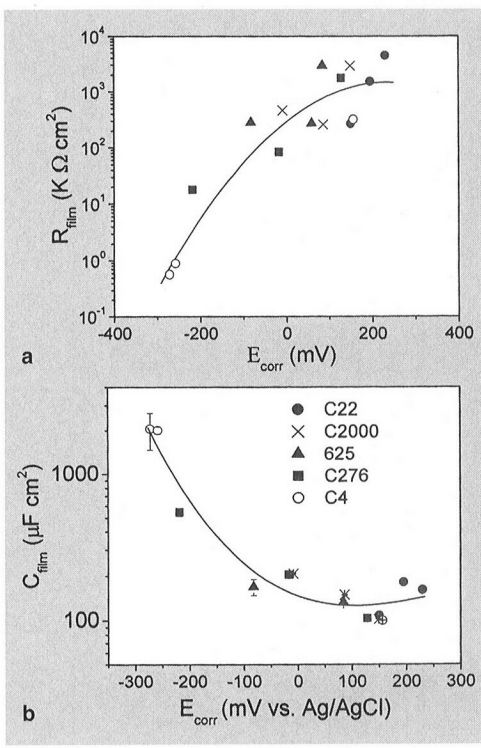

Figure 6. (a) The resistance values of the oxide films (R_{film}) determined from fitting the EIS obtained at open-circuit for all alloys. (b) The capacitance values of the oxide films (C_{film}) determined from fitting the EIS obtained at open-circuit for all alloys.

and a critical threshold potential, E_{crit}. A material is deemed susceptible to the initiation of localized corrosion if $\Delta E = E_{corr} - E_{crit}$ is greater than 0. Even if this criterion is not met, the magnitude of ΔE is taken as an index of localized corrosion resistance (i.e., a more negative value of ΔE represents a greater resistance to localized corrosion). However, the E_{corr}/EIS measurements presented here show that an increase in E_{corr}, termed ennoblement, is coupled to changes in the oxide structure and composition that are beneficial to the protectiveness of the oxide film.

The film-thickening process accompanying ennoblement leads to chromium enrichment at the alloy/oxide interface and the suppression of the defect injection process at this interface. This annealing controls the electronic properties of the film and can lead to extremely low dissolution rates depending on how effectively it is formed (i.e., C-22 vs. C-4). The annealing process appears to be facilitated by the ability of the high-valency cations such as molybdenum and tungsten to retard the transport of cationic defects as the potential increases. This is in contrast to the traditional perspective that the ennoblement of E_{corr} indicates a destabilization of the oxide film. If localized corrosion is to initiate, then the value of E_{crit} must be sufficiently low that the criterion $\Delta E = E_{corr} - E_{crit} > 0$ can be met while the defect concentration of the oxide remains unannealed. This would require a more aggressive environment than that used in these experiments.

CONCLUSIONS

While the open-circuit corrosion behavior of the C alloys and 625 are difficult to separate at 25°C, at 75°C the high-chromium alloys exhibit E_{corr} values that are 300 to 400 mV more positive than those of the low-chromium alloys. The high-chromium, low-molybdenum alloy, 625, exhibits intermediate behavior.

Anodic polarization at a potential well into the passive region (350 mV) yields passive dissolution currents approximately one order of magnitude lower for the high-chromium alloys than the low-chromium alloys. Anodic oxidation yields a passive current for 625 typical of a high-chromium alloy. E_{corr} measurements after anodic oxidation indicate that the passive films present on the high-chromium alloys are stable in the pH = 1 solution at 75°C, whereas the film on the low-chromium C-4 alloy is not. By contrast, the tungsten content of C-276 appears to stabilize the oxide on this alloy. Various measurements show that the film resistance increases and defect concentration decreases as the oxide film thickens and chromium and molybdenum segregate to the alloy/oxide interface and the oxide/solution interface, respectively. These measurements demonstrate that the more positive the value of E_{corr}, the higher the film resistance and the lower its defect density (i.e., the ennoblement in E_{corr} is coupled to the Cr/Mo segregation process and the suppression of defect injection at the alloy/oxide interface).

Thus, by all measures (film resistance, defect concentration and thickness, extent of Cr/Mo segregation, and passive current), the alloy C-22 exhibits the best passive properties.

References

1. Office of Civilian Radioactive Waste Management, Yucca Mountain Project, *www.ocrwm.doe.gov/ymp.*
2. J.R. Myers, F.H. Beck, and M.C. Fontana, *Corrosion*, 21 (1965), p. 277.
3. A.P. Bond and H.H. Uhlig, *J. Electrochemical Society*, 107 (1960), p. 488.
4. G. Lorang et al., *Surface and Interface Analysis*, 16 (1990), p. 325.
5. T. Jabs, P. Borthen, and H.-H. Strehblow, *J. Electrochemical Society*, 144 (4) (1997), p. 1231.
6. P. Marcus and V. Maurice, *Passivity and Its Breakdown*, ed. P. Natishan et al., PV 97-26 (Pennington, NJ: The Electrochemical Society, 1998), p. 254.
7. S.P. Jeng, P.H. Holloway, and C.D. Batich, *Surface Science*, 227 (1990), p. 278.
8. R. Goetz and D. Landolt, *Electrochimica Acta*, 29 (1984), p. 667.
9. L. Zhang and D.D. Macdonald, *Electrochimica Acta*, 43 (18) (1998), p. 2661.
10. M. Bojinov et al., *Electrochimica Acta*, 46 (2001), p. 1339.
11. L. Wegrelius, F. Falkenberg, and I. Olefjord, *J. Electrochemical Society*, 146 (1999), p. 1397.
12. C.R. Clayton and I. Olefjord, *Corrosion Mechanisms in Theory and Practice*, ed. P. Marcus and J. Oudar (New York: Marcel Dekker Inc., 1995), p. 175.
13. G. Bojinov et al., *Electrochimica Acta*, 45 (2000), p. 2029.
14. M. Betova et al., *Electrochimica Acta*, 46 (2001), p. 3627.
15. M. Bojinov et al., *J. Electroanalytical Chemistry*, 504 (2001), p. 29.
16. M. Bojinov, P. Kinnunen, and G. Sundholm, *Corrosion*, 59 (2) (2003), p. 91.
17. A.C. Lloyd et al., *Electrochimica Acta*, 49 (17-18) (2004), p. 3015.
18. A.C. Lloyd et al., *J. Electrochemical Society*, 150 (4) (2003), p. B120.
19. D. Briggs and M.P. Seah, *Practical Surface Analysis by Auger and Photoelectron Spectroscopy* (Toronto, Canada: Wiley, Toronto, 1983), p. 111.

A.C. Lloyd is a corrosion scientist with Kinectrics, Inc. in Toronto, Canada. J.J. Noël is a research associate/adjunct professor and D.W. Shoesmith is a professor with the Department of Chemistry at the University of Western Ontario in London, Canada. N.S. McIntyre is the director of Surface Science Western at the University of Western Ontario in London, Canada.

For more information, contact D.W. Shoesmith, University of Western Ontario, Department of Chemistry, London, Canada, N6A 5B7; (519) 661-2111, ext. 86366; fax (519) 661-3022; e-mail dwshoesm@uwo.ca.